2014

Heat Transfer Characteristics of the Non-uniform Grooved Tube considering Tube Expansion

Sangmu Lee
Shizuoka Works, Mitsubishi Electric Corporation, Japan, Lee.Sangmu@db.MitsubishiElectric.co.jp

Akira Ishibashi
Living Environment Systems Laboratory, Mitsubishi Electric Corporation, Japan, Ishibashi.Akira@ab.MitsubishiElectric.co.jp

Takuya Matsuda
Living Environment Systems Laboratory, Mitsubishi Electric Corporation, Japan,
Matsuda.Takuya@ds.MitsubishiElectric.co.jp

Heat Transfer Characteristics of the Non-Uniform Grooved Tube Considering Tube Expansion

Sangmu LEE[1]*, Akira ISHIBASHI[2] and Takuya MATSUDA[2]

[1]Shizuoka Works, Mitsubishi Electric Corporation, Japan
* E-mail: Lee.Sangmu@db.MitsubishiElectric.co.jp

[2]Living Environment Systems Laboratory, Mitsubishi Electric Corporation, Japan

ABSTRACT

A plate-fin heat exchanger is a type of heat exchanger widely used in air conditioners, and tubes and fins are tightly assembled by the mechanical expansion process of tubes. The tube expansion process deforms the grooves inside the tube, and the groove shapes also affect the adhesion between tubes and fins. In this study, the adhesion and heat transfer performance affected by the tube expansion of the non-uniform grooved tube with different heights are investigated by both analysis and experiments. From the analysis method, it was shown that the contact pressure of non-uniform grooved tube is higher than that of the uniform grooved tube, and the most appropriate high groove number of the non-uniform grooved tube is designed for the maximum contact pressure. From the experimental results, the decreasing rate of the condensation heat transfer coefficient is smaller in the non-uniform grooved tube with different heights, compared to the conventional uniform grooved tube. Also, the air side heat transfer coefficient of the non-uniform grooved tube with different heights is higher than that of the uniform grooved tube.

1. INTRODUCTION

In the manufacturing process of the heat exchanger for air-conditioning system, plate fins are attached to tube by expanding the tube mechanically into the fin collar. As a result, a discontinuity in the region where plate fins attach to the round tube surface introduces a thermal resistance between fins and tube. Compared to the overall thermal resistance, the thermal resistance between fins and tubes cannot be disregarded(Jeong *et al*., 2006). The tube expansion process deforms the grooves inside the tube, and the groove shapes also affect the condensation heat transfer. The heat transfer performance affected by the tube expansion and the effects of the groove shapes on the plate-fin heat exchanger are investigated by experiments(Sasaki *et al*., 2004, Tang *et al*., 2009). But there is no report that considers the contact state between the grooves shape inside the tube and the shape of fin collar by numerical analysis. First, in this study, the analysis on the tube expansion of the uniform grooved tube with same heights is carried out. Second, the adhesion affected by the tube expansion of the non-uniform grooved tube with different heights is investigated by analysis. The optimal number of the non-uniform grooved tube is investigated and the air side heat transfer coefficient of the non-uniform grooved tube with different heights is evaluated.

2. NUMERICAL ANALYSIS

2.1 Calculated Model

Three-dimensional nonlinear calculation for numerical analysis was carried out using commercial structural analysis software ANSYS(Lee *et al.*, 2011). As shown in Fig. 1, the plate-fin heat exchanger broadly used for air-conditioning system is manufactured by the following process. First, the tube is inserted into the fin collar. Second, with the expanding bullet moving forward, the fin collar is enlarged by the expanded outer diameter of the tube. The calculation model is consisted of three parts: tube, 3 layers of fins, expanding bullet as shown in Fig. 2. The grooved tube is modeled with the 90deg domain in the circumferential direction using the symmetry plane. The aluminum fin is a disk-like model. As a boundary condition, both ends of the tube as well fins are constrained in direction of tube axis. Because the tube is restrained so that it may not shrink in the manufacturing process of the heat exchanger and fin collars allow contact between fins. The friction between fin and tube is set as zero. The restriction condition is given so that a fin may not move forward by the slope formed in the expanding process. It is

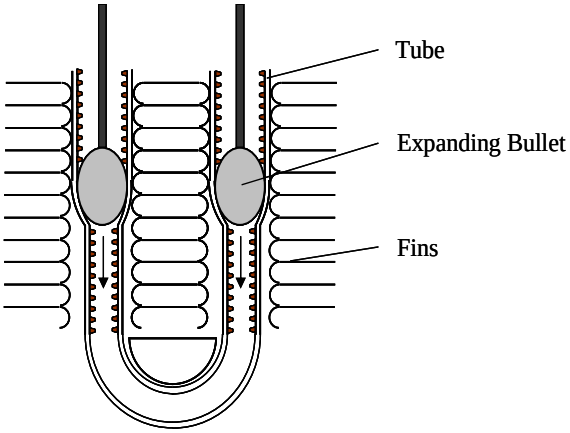

Fig.1 Schematic diagram of tube expansion process

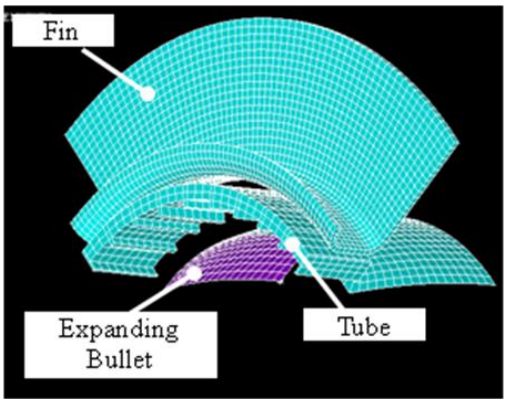

Fig.2 Schematic diagram of calculation model

given as periodic boundary condition that the tube and fin in the circumference cross-section direction are symmetrical structure. The expanding bullet is assumed to be a rigid body. Surface to surface contact is set among tube and fin. Table 1 shows the mechanical properties applied to tube and fins. The materials of the tube and fins are copper and aluminum, respectively. The yield condition assumed the function of isotropic yield by the von Mises type. The hardening condition assumed as isotropic hardening. The stress-strain is obtained through curve fitting method from the material date of pure copper and aluminum(Suzuki *et al.*, 1968).

The geometry parameters of structures in the numerical analysis are given in Table 2. The tested tube is the uniform tube with same height groove and four kinds of non-uniform tube with different height groove. The calculations are carried out with the groove number of high height varying from 4 to 20.

Table 1 Material Properties.

Structure	Tube	Fin
Material	Copper	Aluminum
Young's Modulus [MPa]	110000	70000
Poisson's ratio	0.3	0.3

Table 2 Configurations of Tube and Fin.

Structure		Tube
Outer diameter	[mm]	7.0
Wall thickness	[mm]	0.22
Groove Height	[mm]	0.15
Groove Number (high/low)	[-]	60, 4/44, 12/36, 16/32, 20/40
Structure		Fin
Hole diameter	[mm]	7.26
Fin thickness	[mm]	0.11

2.2 Calculated Result

To evaluate numerical analysis method, firstly, the analysis on the tube expansion of the uniform grooved tube with same heights is carried out with outer diameter of expanding bullet varying from 6.63 to 6.75. The outer diameter, thickness, and groove height of tube is set as 7mm, 0.22mm and 0.15mm, respectively. Fig. 3 shows the influences of expanding bullet's outer diameter on the value of both the outer diameter and thickness. The outer diameter of tube increases with the increasing of outer diameter of expanding bullet. But the thickness of tube decreases because the tube is restrained so that it may not shrink in the manufacturing process of the heat exchanger. Fig. 4 shows the effect of expansion ratio, $\varepsilon/\varepsilon_{0,}$ on the the average contact pressure of the expanded outer surface of the uniform grooved tube. The average contact pressure increase with the increasing of expansion ratio $\varepsilon/\varepsilon_{0.}$ After having shown

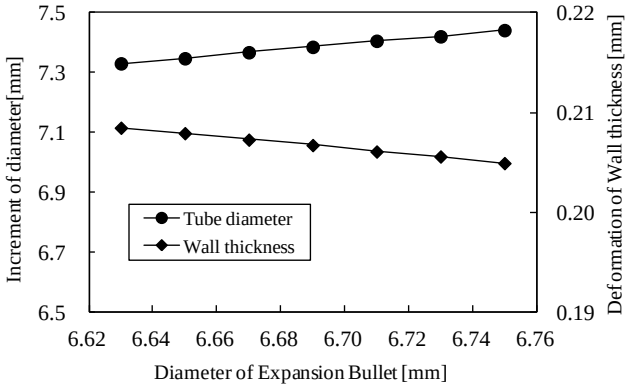

Fig. 3 Effect of Expansion Bullet

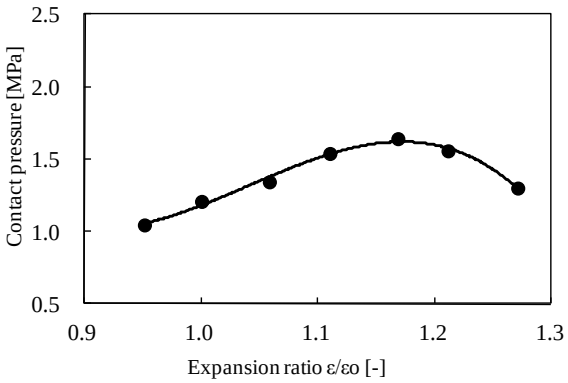

Fig. 4 Contact Pressure after tube expansion

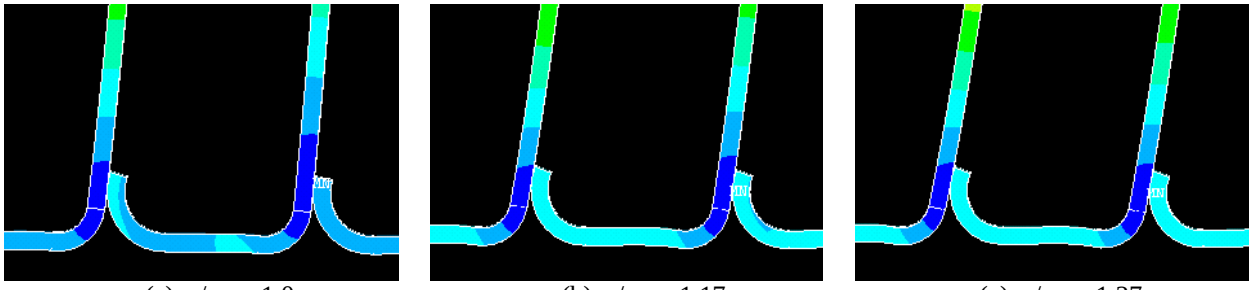

(a) $\varepsilon / \varepsilon_0 = 1.0$ (b) $\varepsilon / \varepsilon_0 = 1.17$ (c) $\varepsilon / \varepsilon_0 = 1.27$

Fig. 5 Cross Section of Fin collar after tube expansion

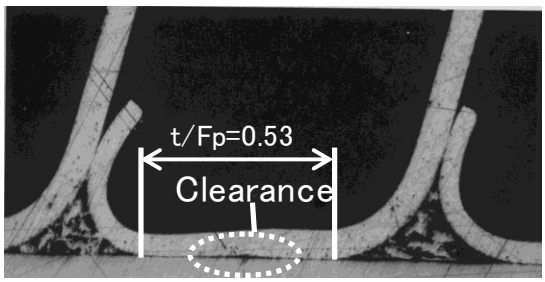

Fig. 6 Section photograph in contact part of fin and tube

the maximum in the expansion ratio $\varepsilon/\varepsilon_0$ 1.17, it decreases. Fig. 5 shows the crosssection of the fin collar with expansion ratio $\varepsilon/\varepsilon_0$ varying. As shown in Fig. 5, there is a gap in the center of the fin collar with the increasing of expansion ratio $\varepsilon/\varepsilon_0$. This result has same characteristic from the contact state between the fin collar and the outer surface of tube, as shown in Fig.6(Ishibashi *et al.*, 2008).

The adhesion affected by the tube expansion of the non-uniform grooved tube with different heights is investigated by analysis. The simulations are carried out with the high groove number varying from 4 to 20. Fig. 7 shows the effect of groove number on the average contact pressure of the expanded outer surface of the uniform grooved tube and non-uniform grooved tube. If the high groove number of non-uniform tube increases, the average contact pressure increases. After having shown the maximum in the high groove number 16 of non-uniform tube, it decreases. Fig. 8 shows the stress distribution in the uniform tube. The height of the uniform tube toward contact with the expanding bullet is about the same. Consequently, the stress distribution is made uniform over the entire contact area of outer surface. Fig. 9(a), (b), (c) and (d) show the stress distribution in the non-uniform tube with the high groove number varying from 4 to20. The point where the expanding bullet touches decreases if there are few high groove numbers as shown in Fig. 9. As a result, the average contact pressure decreases and the thermal contact heat transfer decreases. On the other hand, the point where the expanding bullet touches increases if there are many high groove numbers. The springback of the non-uniform tube is minimized exists and the thermal contact heat transfer becomes maximum.

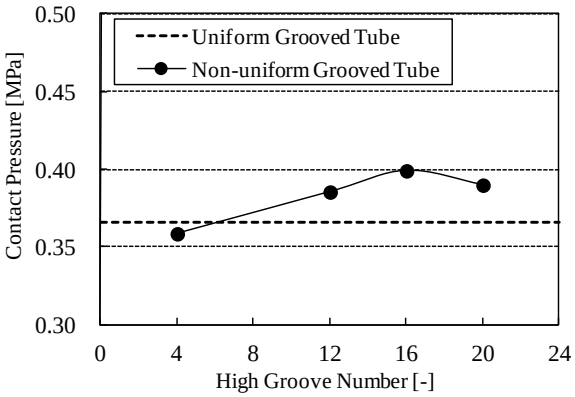

Fig. 7 Contact Pressure after tube expansion

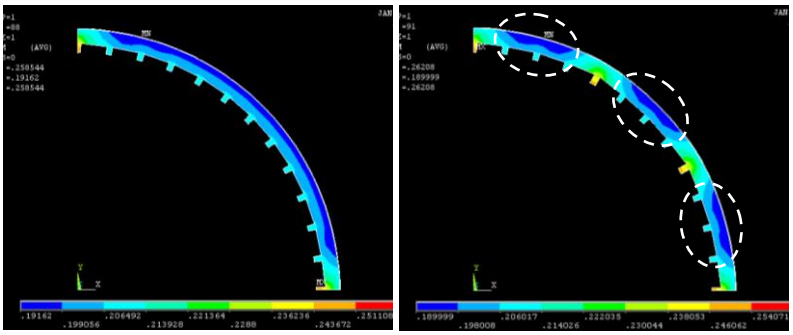

(a) 4 high grooves fin (b) 12 high grooves fin

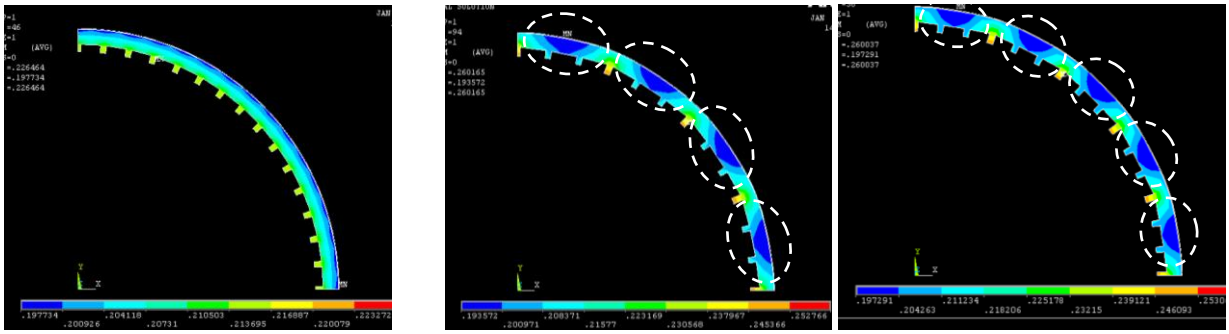

(c) 16 high grooves fin (d) 20 high grooves fin

Fig. 8 Cross Section of the uniform tube after tube expansion

Fig. 9 Cross Section of the non-uniform tube after tube expansion

3. EXPERIMENT

To vakidate of the analysis result, experiments on the refrigerant side heat transfer and the air side heat transfer coefficient are carried out using the uniform grooved tube and most appropriate high groove number of the non-uniform grooved tube. The experimental apparatus, method and tested heat exchanger used in this study is explained.

3.1 Experimental Apparatus For The Refrigerant Side Heat Transfer

Fig. 10 shows the schematic view of the experimental apparatus for measuring the refrigerant side heat transfer, which consists of two loops: a refrigerant loop and a water loop. The refrigerant loop is a typical vapor-compression cycle. The superheated vapor of R410A refrigerant enters compressor through an oil separator, a mixing chamber, a preheater, a test section, an accumulator, a refrigerant mass flow meter, an expansion valve, pre-heater, and a superheater. The lubricant oil used in this apparatus is a kind of POE. It is confirmed that the oil concentration is less than 0.2%. Fig. 11 shows the schematic diagram of the test section for measuring the heat transfer. The test section

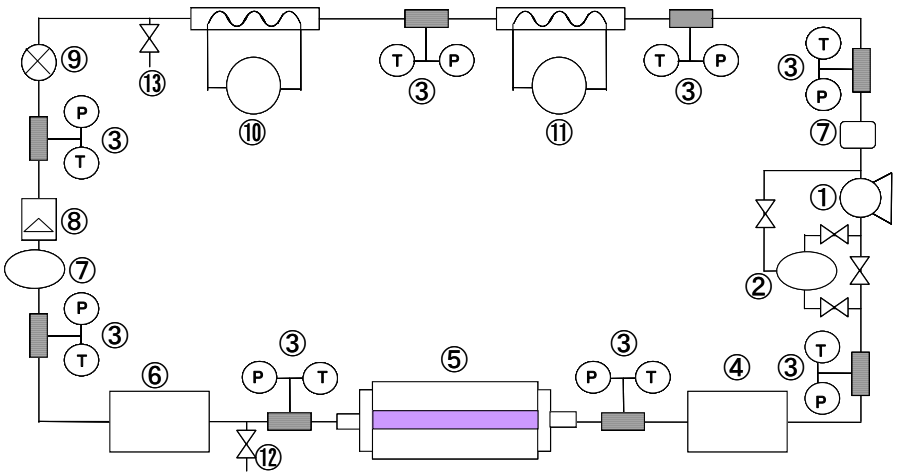

1	compressor
2	oil separator
3	mixing chamber
4	preheater
5	test section
6	subcooler
7	accumulator
8	refrigerant mass flow meter
9	expansion valv e
10	preheater
11	superheater
12	sampling port

Fig. 10 Schematic View of Test Loop

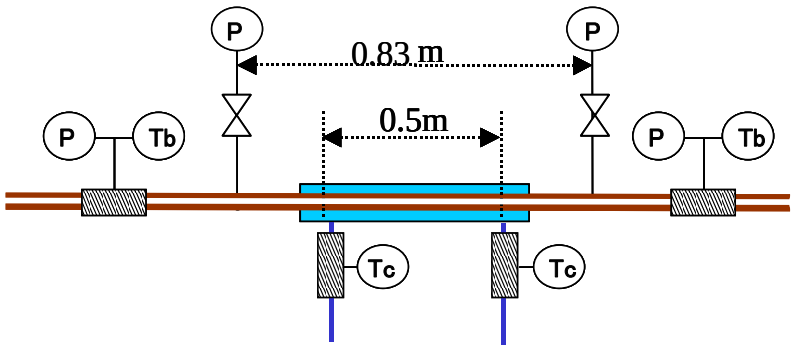

Fig. 11 Schematic of Test section

is double-pipe counter-flow heat exchanger, in which the refrigerant R410A flows inside the inner tube and the cooling water flows counter-currently in the outer annulus. The test section is 0.83 m in total length and the hea t transfer effective length is 0.5 m. Table 3 lists the dimensions of the uniform tube and most appropriate high groove number of the non-uniform tube. In each water mixing chamber, a 2.3 mm O.D. resistance thermometer is equipped to measure the bulk cooling water temperature. All of the resistance thermometers are calibrated within an error of ± 0.02 K. The pressure of refrigerant at the outlet of the test section is measured with the gauge pressure transducer with a precision of ± 0.01 MPa. The pressure difference in each subsection of 0.83 m in length is measured using the differential pressure transducer with a precision of ± 0.13 kPa. The flow rate of the refrigerant is measured by using the micro-motion-type mass flow meter with a precision of ± 0.28 kg/h. The flow rate of cooling water is measured using a gear-type flow meter with a precision of ± 1 *l*/h.

Table 3 Dimensions of test tube

Type		Uniform Grooved Tube	Non-Uniform Grooved Tube
Outer Diameter	(mm)	7.00	7.00
Inner Diameter	(mm)	6.56	6.56
Height	(mm)	0.16	0.18/0.14
Fin tip angle	(deg)	15	15/10
Helix angle	(deg)	30	30
Fin number	(-)	60	16/32

The refrigerant heat transfer coefficient α_i in the uniform grooved tube and the non-uniform grooved tube is calculated as,

$$\alpha_i = \frac{1}{1/K_o - 1/\alpha_c}\left(\frac{A_o}{A_i}\right) \qquad (1)$$

The overall heat transfer coefficient K_o and the log-mean temperature difference ΔT_m is defined as,

$$K_o = \frac{Q}{A_o \cdot \Delta T_m} \quad (2)$$

$$\Delta T_m = \frac{(T_i - t_s) - (T_o - t_s)}{\ln((T_i - t_s)/(T_o - t_s))} \quad (3)$$

where A_o is the total heat transfer area on outside, A_i is the heat transfer area on inside tube, Q is the heat transfer rate over the subsection. T_o is the outlet temperature for cooling, T_i is the inlet temperature for cooling, t_s is the saturation temperature for refrigerant.

The heat transfer coefficient α_c (Petukhov and Roizen, 1964) for cooling is calculated as,

$$\alpha_c = Co\left(\frac{\lambda}{D_e}\right)\left(\frac{d_i}{D_o}\right)^{0.16} Nu_G \quad (4)$$

where λ is thermal conductivity, d_i is the outer diameter of inner tube, D_o is the outer diameter of outer annulus, D_e is the hydraulic diameter.

Nusselt number(Gnielinski, 1976) is defined as,

$$Nu_G = \frac{(f/2)(Re - 1000)Pr}{1 + 12.7\sqrt{(f/2)}(Pr^{2/3} - 1)} \quad (5)$$

$$f = 0.079/Re^{0.25} \quad (6)$$

3.2 Refrigerant Side Heat Transfer

Fig. 12 and 13 show a cross sectional view of the the uniform tube and the non-uniform tube before the tube expansion and after the tube expansion. In the case of the uniform grooved tube, the expanding bullet touches the groove during the tube expansion process causing the grooves inside the tube to deform. On the other hand, in the case of the non-uniform grooved tube, the expanding bullet only touch the high groove. Thus, the high grooves inside the tube is deformed. Fig. 14 shows the decreasing rate of condensation heat transfer on the the uniform tube and the non-uniform tube before the tube expansion and after the tube expansion. In the high quality, the decreasing rate of condensation heat transfer is high. It become small with the decrease of quality. And it can be seen that the decreasing rate of the condensation heat transfer coefficient is smaller in the non-uniform grooved tube. This reason is the difference of liquid film thickness on top of groove height inside the tube.

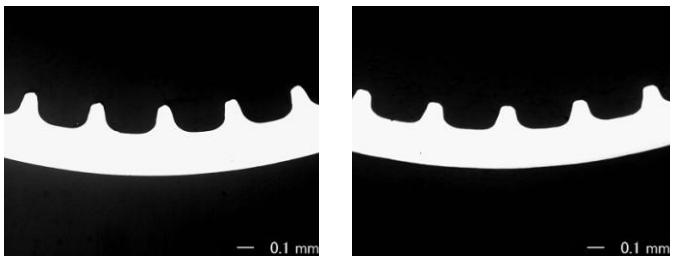

(a) before tube expansion (b) after tube expansion

Fig. 12 Cross Section of Uniform Grooved Tube

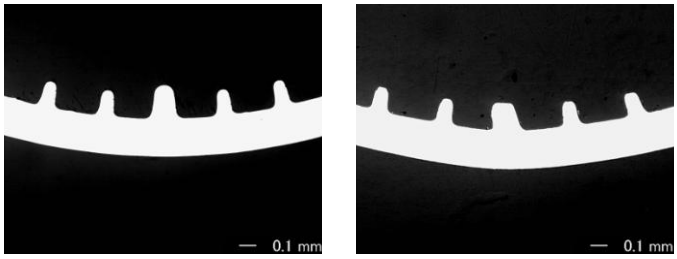

(a) before tube expansion (b) after tube expansion

Fig. 13 Cross Section of Non-uniform Grooved Tube

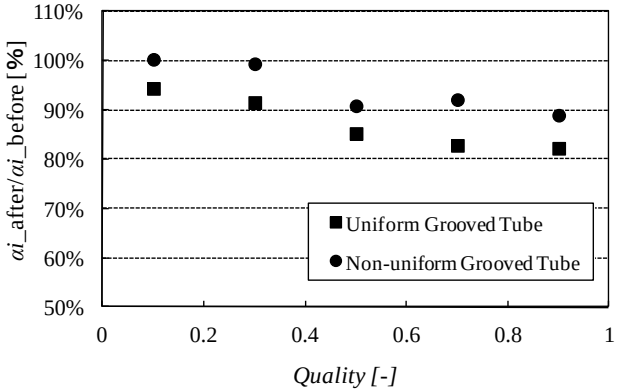

Fig. 14 Heat transfer coefficient of Inner Grooved Tube

3.3 Experimental Apparatus For Air Side Heat Transfer

Fig. 15 shows the schematic view of the experimental apparatus for measuring the air side heat transfer. The tested heat exchanger is setted in wind tunnel, which is installed in the room of constant air temperature and constant air humidity. A wind tunnel has a 300x300mm opening, which consists of an upstream honeycomb, an upstream air sampling tree, an upstream thermocouple grid, a tested heat exchanger, a downstream honeycomb, a downstream air sampling tree, a downstream thermocouple grid, flow nozzle, and a fan. The heating water flow into the inner tube of a tested heat exchanger. In each water mixing chamber, a 2.0 mm O.D. resistance thermometer is equipped to measure the bulk heating water temperature. The flow rate of heating water is measured using a gear-type flow meter. The inlet and outlet temperature of the air stream is measured with twenty copper-constantan thermocouples, arranged 4x5 uniformly on the cross sectional area of the air duct. The flow nozzle was used to measure the air flow rate inside the tested heat exchanger. The specifications of the tested heat exchanger in the experiment are given in Table 4.

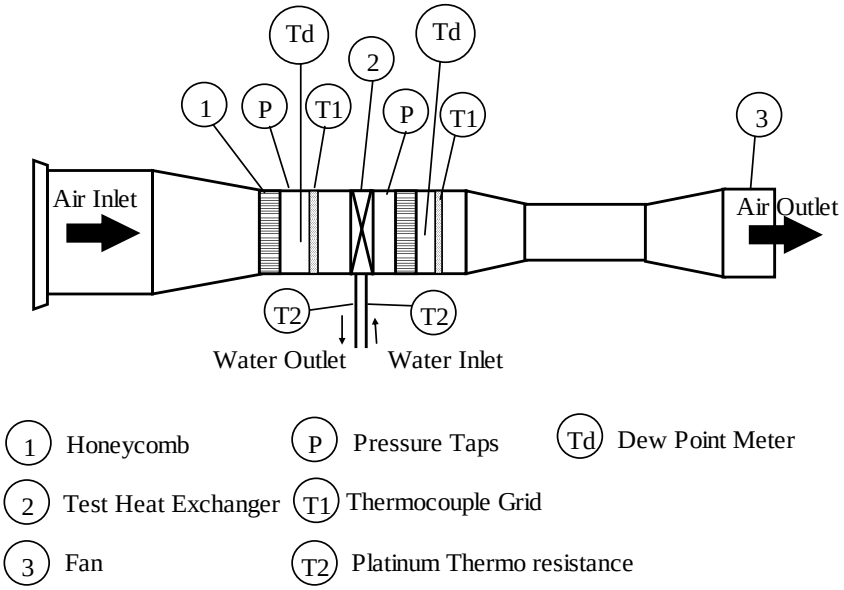

Fig.15 Experimental Apparatus

Table 4 Specifications of Tested Heat Exchanger.

Tube Diameter	[mm]	7.0
Tube Wall thickness	[mm]	0.22
Transversal Tube Pitch	[mm]	21
Longitudinal Tube Pitch	[mm]	22
Number of Row	[-]	1
Fin Pitch	[mm]	1.3
Fin thickness	[mm]	0.11

Table 5 Experimental Conditions.

Inlet Temperature of Air	[°C]	20
Air Velocity	[m/s]	1.0,1.5,2.0
Fluid		Heating Water
Flow Rate	[L/min]	4, 6, 8, 10
Inlet Temperature of Fluid	[°C]	50

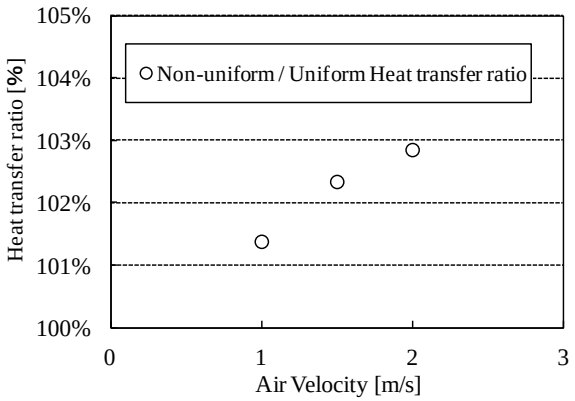

Fig.16 Air heat transfer coefficient

Experimental test conditions for tested heat exchanger were tabulated in Table 5. The inlet temperature of air side conditions were 20 °C(dry bulb). The inlet temperature of heating water side conditions were 50 °C. The air velocity vary from 1 to 2 m/s and the flow rate of the heating water vary from 4 to 10 L/min. Changing the air velocity and the heating water flow rate, the air side heat transfer is calculated using Wilson Plot Method. The uncertainty of heat transfer rate is less than 2.5%.

3.4 Air Side Heat Transfer

Fig. 16 shows the effect of air velocity on the air heat transfer coefficient with the uniform grooved tube and non-uniform grooved tube. The air heat transfer coefficient of non-uniform grooved tube is 1.4% higher than that of the uniform grooved tube in case of air velocity 1 m/s. This might be caused by the increase of the average contact pressure in the non-uniform tube. It is also seen from Fig. 16 that the difference values between the uniform grooved tube and non-uniform grooved tube increase with the increase of air velocity especially. This result implies that the thermal contact resistance makes up a large percentage of the overall thermal resistance value with the increase of air heat transfer coefficient.

6. CONCLUSIONS

In the manufacturing process of the heat exchanger for air-conditioning system, the analysis on the tube expansion when attaching the fin collar to the tube by mechanical method carried out to evaluate the adhesion between tubes and fins on the uniform tube with same height groove and four kinds of non-uniform tube with different height grooves. From the analysis method, it was shown that the average contact pressure become maximum in the high groove number 16 of non-uniform tube. From the experimental results, the decreasing rate of the condensation heat transfer coefficient is smaller in the non-uniform grooved tube with different heights, compared to the conventional uniform grooved tube. Also, the air side heat transfer coefficient of the non-uniform grooved tube with different heights is higher than that of the uniform grooved tube.

NOMENCLATURE

A_i	heat transfer area on inside [m^2]
A_o	heat transfer area on outside [m^2]
D_e	hydraulic diameter [mm]

D_o	outer diameter of outer annulus [mm]
d_i	outer diameter of inner tube [mm]
f	friction factor [-]
K_o	overall heat transfer coefficient [W/m^{2}K]
Nu	Nusselt number [-]
Pr	Prandtl number [-]
Q	heat transfer rate [W]
Re	Reynolds number [-]
T_i	inlet temperature for cooling [K]
T_o	outlet temperature for cooling [K]
t_s	saturation temperature for refrigerant [K]
ΔT_m	log-mean temperature difference [-]

Greek symbols

α_i	heat transfer coefficient for refrigerant [W/m^{2}K]
α_c	heat transfer coefficient for cooling [W/m^{2}K]
ε	expansion ratio [-]
ε_o	conventional expansion ratio [-]
λ	thermal conductivity [W/mK]

REFERENCES

Jeong, J., Kim, C. N., and Youn, B., 2006, A study on the thermal contact resist in fin-tube heat exchanger with 7mm tube, *Int. J. Heat and Mass Transfer*., vol. 49, No. 7, pp. 1547-1555.

Sasaki, N., Kakiyama, S. H., and Sanuki, N., 2004, Effect of enhanced heat transfer spirally grooved tube with ability to control the heat transfer disturbance by mechanical tube expanding, *Trans. of the JSRAE*, Vol. 21, No. 2, pp. 129-138.

Tang, D., Peng, Y., and Li, D., 2009, Numerical and experimental study on expansion forming of inner grooved tube, *Journal of Materials Processing Technology*, Vol. 209, pp. 4668-4674.

Lee, S., Ishibashi, A., and Matsuda, T., 2011, Heat transfer characteristics of high performance inner grooved tube, *Proc. JSRAE Annual Conference*., Tokyo, pp. 503-504

Suzuki, H., Hashizume, S., Yabuki, Y., Ichihara, Y., Nakajima, S., and Kenmochi, K., 1968, *Report of the Institute of Industrial Science*, The University of Tokyo, Vo.18, No.3.

Ishibashi, A., Kaga, K., Mukouyama, T., and Tadokoro, T., 2008, Design of compact heat exchanger for air conditioner indoor unit, *Proc. JSRAE Annual Conference*., Osaka, pp. 77-80.

Petukhov, B. S. and Roizen, L. I., 1964, Generalized relationships for heat transfer in a turbulent flow of a gas in tubes of annular section, High temperature(USSR), Vol. 2, pp. 65-68.

Gnielinski, V., 1976, New equations for heat and mass transfer in turbulent pipe channel flow, *International Chemical Engineering*, Vol. 16, No. 2, pp. 359-368.

ACKNOWLEDGEMENT

The test tubes were kindly provided by Kobelco and Materials Copper Tube, Ltd.